Charge Effects and Josephson Plasma Resonance on Planar Defects in High-Temperature Superconductors

A. Gurevich[1] and M. Tachiki[2]
[1]*Applied Superconductivity Center, University of Wisconsin, Madison, Wisconsin 53706*
[2]*National Research Institute for Metals, 1-2-1 Sengen, Tsukuba 305-0047, Japan*
(Received 9 November 1998)

We show that planar crystalline defects parallel to the ab planes in high-T_c superconductors (HTS) give rise to a localized Josephson plasma mode formed by a collective Coulomb interaction of interlayer junctions. This results in a pronounced satellite line in the real part of the complex resistivity $R(\omega)$, whose position and amplitude depend on the critical current density J_0 and on the parameters of the charge interlayer coupling. The narrowness of the zero-field plasma peak in Re$R(\omega)$ enables one to probe the pairing symmetry of the interplane coupling by extracting the angular dependence of $J_0(\theta)$ across twist grain boundaries in HTS bicrystals.

PACS numbers: 74.60.Ge

Weak Josephson coupling of the Cu-O planes in high-temperature superconductors (HTS) can manifest itself in steps on the voltage-current characteristics along the c axis [1] and in a weakly damped Josephson plasma mode with the frequency ω_p smaller than the superconducting gap Δ [2–4]. The plasma mode gives rise to a narrow peak in the real part of the complex resistance $R(\omega)$ at low temperatures T for which the quasiparticle damping is suppressed. A sharp peak in Re$R(\omega, H, T)$ has also been observed on Bi-2212 single crystals in a dc magnetic field H [5–7] when the Josephson plasma line is broadened due to vortices. In this case the dependence Re$R(H)$ at high fields carries information about the vortex correlation function in the liquid state [8].

In this paper, we show that the narrowness of the zero-field Josephson plasma line and its sensitivity to the local interlayer coupling could also make the Josephson plasma resonance a very useful technique for studying planar crystalline defects parallel to the ab planes, such as twist grain boundaries (GB) and stalking faults in Bi-2212 crystals. Because of the short coherence length along the c axis, planar defects can strongly reduce the interlayer supercurrent density, J_c, affecting, for example, the structure of Josephson vortices parallel to the ab planes [9]. Therefore, understanding the nature of interlayer coupling also requires a nondestructive way of identifying and characterizing planar defects in order to separate their contribution from intrinsic mechanisms.

Current transport along the c axis can be strongly impeded by planar defects, which is a serious problem for power applications of HTS [10]. If the c-axis current density J exceeds the supercurrent density J_0 across the defect, it switches into a resistive state and also induces local voltages V_n on neighboring layers with $J_c > J_0$ coupled by the screened Coulomb interaction [11]. For $J_0 \simeq J_c$, transport measurements may therefore not reveal the true J_0, due to the admixture of quasiparticle currents induced on other layers with $J_c > J_0$. For instance, recent resistive measurements [12] indicated that twist GBs did not noticeably reduce the apparent interlayer critical current density $J_0(\theta)$ which showed weaker dependence on the misorientation angle θ between the adjacent crystallites than that expected from the d-wave x^2-y^2 pairing symmetry. This behavior of twist GBs is also in sharp contrast with in-plane tilt GBs, which exhibit the rapid exponential decrease $J_c \propto \exp(-\theta/\theta_0)$, $\theta_0 \sim 4°–5°$ [13] due to charging effects and the proximity of HTS materials to the metal-insulator transition [14,15]. Understanding the mechanisms of current transport through twist GBs and extracting the intrinsic $J_0(\theta)$ dependence is therefore very important for clarifying the symmetry of the interplane superconducting coupling. We show that the narrowness of the Josephson plasma line in principle enables one to circumvent the limitation of resistive measurements at $J_0 \simeq J_c$ and to reveal a true J_0 of a single GB coupled with other interlayer junctions.

We consider a layered HTS in ac magnetic field parallel to the ab plane and zero dc magnetic field H. In this case vortices are absent, and the ac electric field E_ω is induced only along the c axis. We also assume that a c-axis dc bias current density J is applied, which enables one to control the Josephson plasma frequency ω_p by varying J:

$$\omega_p = \left(\frac{8\pi^2 cdJ_c}{\phi_0\epsilon}\right)^{1/2}\left(1 - \frac{J^2}{J_c^2}\right)^{1/4}. \qquad (1)$$

Here ϵ and d are the dielectric constant and the thickness of the block layer between the superconducting layers, ϕ_0 is the flux quantum, and c is the speed of light.

The electrodynamics of a layered HTS is described by coupled nonlinear equations for the phase differences $\varphi_n(t)$ between the $(n+1)$th and nth superconducting layers, where $-N < 2n < N$, and N is the total number of layers. The coupling between different interlayer junctions can be due to magnetic interaction of supercurrents flowing along different layers [4], Coulomb interaction due to

 © 1999 The American Physical Society

charge redistribution between the layers [11], or current-induced particle-hole asymmetry [16]. In this paper we take into account only the Coulomb coupling of the interlayer junctions and neglect their magnetic interaction, since no currents flow along the layers at $H = 0$. The particle-hole asymmetry can also be neglected for layered HTS with very high c-axis resistivity characteristic of Bi-2212 crystals [16]. We consider linear response to a small ac signal and calculate the complex resistance $R(\omega)$ for a stack of N layers which contains one interlayer junction with reduced critical current density $J_0 < J_c$. The planar defect gives rise to the localized plasma mode with the frequency ω_0 smaller than the bulk ω_p. The localized mode is formed by a collective Coulomb interaction of many ($\sim 10-10^2$) interlayer junctions near the defect, so the amplitude of the satellite peak in $\mathrm{Re}R(\omega_0)$ is much higher than $R(\omega_0) \sim R(\omega_p)/N$ for decoupled junctions. In this case by measuring the satellite peak, one can extract J_0 and the in-plane screening length r_D, which determines the charge coupling of the ab planes [11]. Besides, r_D is a key parameter of the strong electric field effects in HTS, which contribute to the suppression of Δ on tilt GBs and current transport through GBs in the ab plane [14,15].

The equations for $\varphi_n(t)$ for a stack of coupled Josephson junctions have the form [11]

$$C_n \dot{V}_n + G_n V_n + J_{cn} \sin\varphi_n = J(t), \tag{2}$$

$$V_n - \alpha(V_{n+1} + V_{n-1} - 2V_n) = \hbar\dot{\varphi}_n/2e, \tag{3}$$

where $J(t)$ is the external current density perpendicular to the layers, J_{cn} is the tunneling supercurrent density, V_n is the local voltage between the $n+1$ and nth layers of thickness s spaced by d, $\alpha = r_D^2/sd$ is the charge coupling parameter, $C = \epsilon/4\pi d$ is the specific interlayer capacitance, G is the interlayer quasiparticle conductance per unit area, and the overdot denotes time derivative. For $s = 3$ Å, $d = 12$ Å, $r_D \simeq 5-10$ Å [15], we obtain $\alpha \simeq 1-3$, which indicates strong interlayer Coulomb coupling in HTS.

Now let J_{cn} in Eq. (2) have the same value J_c for all n, but the defect layer with $n = 0$, for which $J_0 < J_c$, $C_0 \neq C$, and $G_0 \neq G$. We consider a small harmonic ac signal $J_\omega \exp(i\omega t)$ superimposed on a dc current J flowing across the stack, $J(t) = J + J_\omega e^{i\omega t}$, for $|J_\omega| \ll J$. Then $\varphi_n = \sin^{-1}(J/J_{cn}) + \delta\varphi_n(\omega)e^{i\omega t}$, and Eq. (2) can be linearized with respect to the induced phase perturbations, $\delta\varphi_n = [J_\omega - (G_n + i\omega C_n)V_n]/\sqrt{J_{cn}^2 - J^2}$. Substituting this into Eq. (3), we obtain the following equation for the Fourier components $V_n(\omega)$:

$$gV_n - \alpha(V_{n+1} + V_{n-1} - 2V_n) = if\beta + ifF\delta_{n0}, \tag{4}$$

where $g(\omega) = 1 - f^2 + i\gamma f$, $f = \omega/\omega_p$, $\beta = \hbar\omega_p J_\omega/2e\sqrt{J_c^2 - J^2}$, $\gamma = \hbar\omega_p G/2e\sqrt{J_c^2 - J^2}$. The parameter F, which describes the influence of the planar defect, is given by

$$F = \eta[\beta - (if + \gamma)V_0], \tag{5}$$

$$\eta = \sqrt{\frac{J_c^2 - J^2}{J_0^2 - J^2}} - 1. \tag{6}$$

Here we assumed for simplicity that C_n and G_n do not change on the defect layer; however, the results can be easily generalized to the case $G \neq G_0$ and $C \neq C_0$. The resistance $R(\omega)$ is determined by even modes $V_n = V_{-n}$, for which the solution of Eq. (4) has the form

$$V_n(f) = \frac{if\beta}{g}\left[1 + \frac{\eta a^{|n|}}{\sqrt{g^2 + 4\alpha g} - \eta f(f - i\gamma)}\right], \tag{7}$$

where $a = 1 + (g - \sqrt{g^2 + 4\alpha g})/2\alpha$. The second term in the brackets in Eq. (7) describes the localized plasma mode $v_n = V_n - V_n^{(0)}$ near GB, where $V_n^{(0)} = if\beta/g$ are induced ac voltages in a uniform sample. If ω is close to ω_p, we have $g(\omega) \ll 1$, and $a = 1 - \sqrt{g/\alpha}$ for $\alpha \sim 1$. In this case the localized voltage perturbation $v_n = v_0 a^{|n|}$ decays on the correlation length $L \simeq (s + d)\sqrt{\alpha/g}$ away from the defect (Fig. 1). For $\gamma = 0$, L is given by

$$L = (d + s)\sqrt{\frac{\alpha\omega_p^2}{\omega_p^2 - \omega^2}}. \tag{8}$$

Near the bulk resonance ($\omega_p - \omega \ll \omega_p$), the decay length L is much larger than the interlayer spacing d. Furthermore, L increases as the charge coupling parameter α and the frequency ω increase, approaching $L \sim (d + s)\sqrt{\alpha/\gamma} \gg d$ for $\omega \to \omega_p$. The fact that $L \gg d + s$ indicates that the localized mode is formed by the Coulomb coupling of many layers (see Fig. 1).

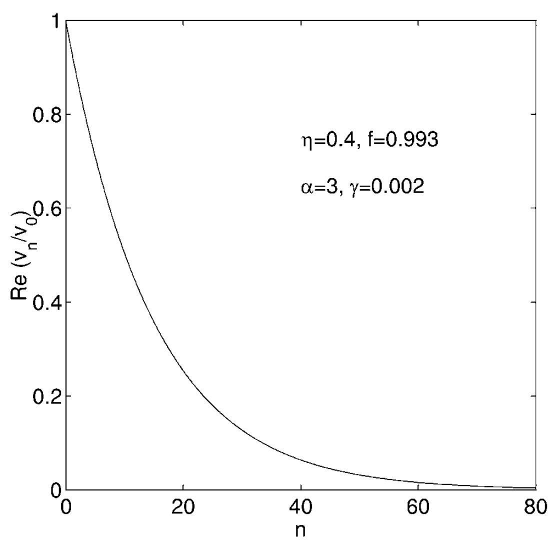

FIG. 1. Localized voltage distribution $v_n/v_0 = \mathrm{Re}(a^{|n|})$ near the defect for $\omega = \omega_0$, $\eta = 0.4$, $\alpha = 3$, and $\gamma = 0.002$.

Now we calculate the complex resistance $R(\omega) = \sum_n V_n/I_\omega$, where I_ω is the Fourier component of the ac current. Assuming $D = N(s + d) \gg 2L$, and summing up Eq. (4) over n, we obtain that $\sum_n V_n = if(N\beta + F)/g$, since the contribution from the terms proportional to α cancels out with an accuracy to $\exp(-D/2L) \ll 1$, where D is the sample thickness. Substituting F and V_0 from Eqs. (5) and (7) into $R = if(N\beta + F)/gI_\omega$, we obtain

$$\frac{R(\omega)}{R_0} = \frac{if}{g}\left[N + \frac{\eta}{g - \eta f(f - i\gamma)/\sqrt{1 + 4\alpha/g}}\right], \tag{9}$$

where $R_0 = \hbar\omega_p/2e\sqrt{I_c^2 - I^2}$. The first term in the brackets corresponds to a uniform sample, and the second term proportional to η describes the contribution of the localized plasma mode near GB. In Eq. (9) we took into account the single defect in the center, but neglected the influence of the sample surfaces, which do not cause any new localized plasma modes at $\omega \simeq \omega_p$ [17,18].

Shown in Fig. 2 is the dissipative part $\mathrm{Re}R(\omega)$, which has peaks at ω_p and ω_0 determined by the poles in $R(\omega)$. Here the bulk plasma frequency, $\omega = \omega_p(1 + i\gamma/2)$, is a solution of $g(\omega) = 0$. The frequency ω_0 of the localized plasma mode satisfies the equation

$$g^2 + 4\alpha g = \eta^2 f^2 (f - i\gamma)^2. \tag{10}$$

Equation (10) reduces to the quadratic equation $g^2 + 4\alpha g = \eta^2(1 - g)^2$, whose solution, $g_0 > 0$, determines the eigenfrequency, $\omega_0/\omega_p = (1 - g_0 - \gamma^2/4)^{1/2} + i\gamma/2$. For $\eta^2 \ll 4\alpha$, and $\gamma \ll 1$, we obtain $g_0 = \eta^2/4\alpha \ll 1$, and

$$\omega_0/\omega_p = 1 - \eta^2/8\alpha + i\gamma/2. \tag{11}$$

For $\alpha = 3$, $J_0 = 0.5J_c$, and $J = 0$, we get $\omega_p - \omega_0 \simeq 4 \times 10^{-2}\omega_p$. Thus, if J_0 is not very different from J_c, the synchronization of many layers near the defect layer gives rise to the eigenfrequency ω_0, which is much closer to ω_p, than one could expect from Eq. (1). For $J \to J_0$, $\eta(J)$ diverges, and ω_0 vanishes at $\eta \to \infty$ and $\gamma = 0$ as

$$\omega_0/\omega_p = (1 + 4\alpha)^{1/4}/\sqrt{\eta}. \tag{12}$$

The case $\eta \gg 1$ also models the sample surface, for which $J_0 \to 0$ and the localized plasma mode is absent [17]. As follows from Fig. 2, the strong Coulomb coupling can make the amplitude of the satellite peak, $R(\omega_0) \sim (2L/D)R(\omega_p)$, quite noticeable. For instance, Eqs. (8) and (11) give $2L(\omega_0)/D \sim 4\alpha/\eta N \sim 0.3$–$0.03$ for $\gamma\omega_p \ll \omega_p - \omega_0$, $\alpha \simeq 3$, $\eta \sim 0.1$–1, and $N \sim 400$, which corresponds to $D \simeq 1\ \mu$m for Bi-2212.

As the damping parameter γ increases, the plasma lines broaden and overlap; thus the satellite peak can be resolved only for weak damping, $\gamma < \gamma_c \simeq \Delta\omega/\omega_p \simeq \eta^2/8\alpha \simeq 4 \times 10^{-2}$ for $\alpha = 3, \eta = 0.5$. Estimates of

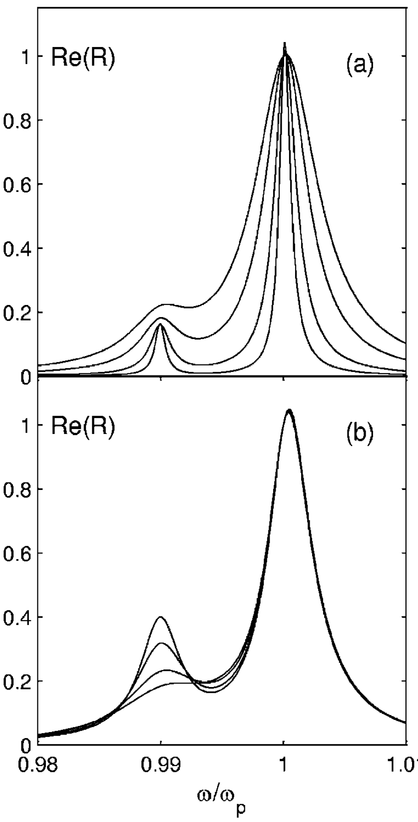

FIG. 2. The effect of dissipation (a) and distribution of local J_0 (b) on the normalized $\mathrm{Re}R(\omega)/R(\omega_p)$, calculated from Eqs. (9) and (16). Figure 2a corresponds to $\alpha = 3$, $\eta = 0.5$, $N = 400$, $\Gamma = 0$, and different $\gamma = 0.001$ (bottom curve), 0.002, 0.004, and 0.006 (top curve). (b) corresponds to $\gamma = 0.004$, $N = 200$, $\alpha = 3$, and different distribution widths $\Gamma = 0$ (top curve), 0.01, 0.03, and 0.05 (bottom curve).

γ for $YBa_2Cu_3O_7$ give $\gamma \sim 0.1$ near T_c [1]; however, γ_c decreases at lower T due to the decrease of density of thermally activated quasiparticles and the c-axis conductivity. For instance, recent measurements of $R(\omega)$ on Bi-2212 crystals at $H = 0$ gave the Josephson plasma linewidth $\delta\omega_p < 10^{-2}\omega_p$ [19], which would be sufficient to resolve the satellite plasma line, whose relative amplitude $R(\omega_0) \sim (2L/D)R(\omega_p)$ can also be increased by decreasing the sample thickness. For instance, for smaller D, say $D \simeq 0.5\ \mu$m, $N = 200$, the satellite peak in $\mathrm{Re}R(\omega)$ becomes more pronounced (Fig. 2b) and can be resolved for larger γ than those in Fig. 2a.

By measuring ω_0 for different J, one can extract J_0 across the defect layer and the parameter α. Using Eqs. (9) and (11), we can express α and J_0 in terms of the observed $\Delta\omega/\omega_p$ for $J = 0$ and for $J \ll J_0$ as follows:

$$\alpha = \left(\frac{J_c}{J_0} - 1\right)^2 \frac{\omega_p(0)}{8\Delta\omega(0)}, \tag{13}$$

$$\frac{J^2}{J_0}\left(\frac{1}{J_0} + \frac{1}{J_c}\right) = \frac{\Delta\omega(J)\omega_p(0)}{\Delta\omega(0)\omega_p(J)} - 1, \tag{14}$$

where $\Delta\omega(J) = \omega_p(J) - \omega_0(J) \ll \omega_p(J)$, and J_c and G can be obtained independently from the amplitude and the width of the bulk Josephson plasma line. Notice that extracting G may be more involved, since the plasma linewidth in HTS crystals can be due to both the quasiparticle damping and the distribution of the interlayer coupling strengths [20] because of long-range chemical inhomogeneities and strains, or inhomogeneous magnetization currents along the c axis at $H > 0$. For an array of planar defects with different J_0, the satellite peaks in $\mathrm{Re}R(\omega)$ overlap, and the averaged resistance

$$\bar{R}(\omega) = \int_0^\infty R(\omega, J_0) P(J_0)\, dJ_0 \tag{15}$$

can be expressed via the distribution function $P(J_0)$, if the mean spacing between the defects is larger than L. Equation (15) also describes a single GB with variations of J_0 along GB on macroscopic scales $\gg L$. As an example, we consider the Lorentzian function $P_0 = \Gamma/(x^2 + \Gamma^2)\pi$, where $x = (J_0 - \bar{J}_0)/\bar{J}_0$, and Γ quantifies the width of the distribution of local J_0 around the mean $\bar{J}_0$. For a narrow distribution, $\Gamma \ll 1$, which does not completely wash out the satellite peak, we can expand $\eta(J_0) = \eta - (\eta + 1)x$ in Eqs. (6) and (9), assuming that $J = 0$, and $\bar{\eta}$ corresponds to $J_0 = \bar{J}_0$. Near the plasma resonance, $\omega \approx \omega_p$, the main contribution in Eq. (15) comes from the region $|x| \ll 1$, where we can extend the integration limits to $-\infty < x < \infty$ and calculate $\bar{R}$ by contour integration in the upper complex half-plane. As a result, $\bar{R}(\omega)$ reduces to Eq. (9) with η replaced by

$$\eta_{\mathrm{eff}} = \bar{\eta} - i(1 + \bar{\eta})\Gamma\,. \tag{16}$$

The evolution of $\mathrm{Re}R(\omega)$ with Γ is shown in Fig. 2b. The amplitude of the satellite peak, $\mathrm{Re}R(\omega_0) \simeq (4\alpha/\eta)^2 R_0/(1 + \eta)\Gamma$, decreases with Γ, if $\Gamma \gg \Gamma_c \sim \gamma(2\alpha + \eta^2)/\eta(1 + \eta) \approx 8.3\gamma$, for $\alpha = 3$ and $\eta = 0.5$. Therefore, the single satellite peak in $\mathrm{Re}R(\omega)$, which carries the information about the superconducting and charge coupling along the c axis, could be resolved in high quality thin Bi-2212 bicrystals, for which the parameters of the twist GB are well quantified and controlled.

In conclusion, measuring the satellite plasma peak in $\mathrm{Re}R(\omega)$ at $\omega_0 < \omega_p$ enables one to extract the charge coupling parameter α and the supercurrent density J_0 across planar defects parallel to the ab planes. This may provide a sensitive tool for probing the pairing symmetry of the interlayer coupling by measuring the angular dependence $J_0(\theta)$ for twist grain boundaries in Bi-2212 bicrystals. If α is independent of θ, the behavior of $J_0(\theta)$ can be obtained directly from Eq. (13).

The work of A. G. was supported by NSF MRSEC Program (DMR 9214707). We are grateful to D. C. Larbalestier and K. Kadowaki for stimulating discussions.

[1] R. Kleiner and P. Müller, Phys. Rev. B **49**, 1327 (1994).
[2] H. A. Fertig and S. Das Sarma, Phys. Rev. Lett. **44**, 4480 (1991); T. Mishonov, Phys. Rev. B **44**, 12 033 (1991).
[3] M. Tachiki, T. Koyama, and S. Takahashi, Phys. Rev. B **50**, 7065 (1994).
[4] L. N. Bulaevski *et al.*, Phys. Rev. B **50**, 12 831 (1994); L. N. Bulaevski, M. P. Maley, and M. Tachiki, Phys. Rev. Lett. **74**, 801 (1995).
[5] O. K. C. Tsui, *et al.*, Phys. Rev. Lett. **73**, 724 (1994); **76**, 819 (1996).
[6] Y. Matsuda *et al.*, Phys. Rev. Lett. **75**, 4512 (1995); Phys. Rev. B **55**, R8685 (1997).
[7] K. Kadowaki *et al.*, Phys. Rev. B **56**, 5617 (1997).
[8] A. E. Koshelev, L. N. Bulaevski, and M. P. Maley, Phys. Rev. Lett. **81**, 902 (1998).
[9] K. A. Moler *et al.*, Science, **279**, 1193 (1998); A. Gurevich *et al.*, Phys. Rev. B **54**, 13 196 (1996).
[10] D. C. Larbalestier, Science **274**, 736 (1996).
[11] T. Koyama and M. Tachiki, Phys. Rev. B **54**, 16 183 (1996).
[12] Y. Zhu *et al.*, Phys. Rev. B **57**, 8601 (1998).
[13] D. Dimos, P. Chaudhari, and J. Mannhart, Phys. Rev. B **41**, 4038 (1990).
[14] A. Gurevich and E. A. Pashitskii, Phys. Rev. B **57**, 13 878 (1998).
[15] J. Mannhart and H. Hilgenkamp, Supercond. Sci. Technol. **10**, 880 (1997); Appl. Phys. Lett. **73**, 265 (1998).
[16] S. N. Artemenko and A. G. Kobelkov, Phys. Rev. Lett. **78**, 3551 (1997); D. A. Ryndyk, *ibid.* **80**, 3376 (1998).
[17] S. Takahashi *et al.*, Physica (Amsterdam) **293C**, 64 (1997).
[18] For finite D, the dispersion of the longitudinal plasma mode results in the resonances at $\omega_n = \omega_p\sqrt{1 + (r_D k_n)^2}$, where $k_n = \pi(2n + 1)/D$, $n = 0, 1, 2, \ldots$ [17]. For $D = 1\ \mu$m and $r_D = 8$ Å, we get $(\omega_1 - \omega_p)/\omega_p \simeq (\pi r_D/D)^2/2 \sim 10^{-6}$. Since $\omega_{n+1} - \omega_n$ is much smaller than both the line width $\gamma\omega_p$ and $\Delta\omega = \omega_p - \omega_0$, the peaks at ω_n strongly overlap, so the size effects can be neglected.
[19] K. Kadowaki *et al.* (unpublished).
[20] D. van der Marel and A. Tsvetkov, Czech. J. Phys. Suppl. S6 **46**, 3165 (1996); J. Schützmann *et al.*, Phys. Rev. B **55**, 11 118 (1997).